Radial Velocity Search for Extrasolar Planets in Visual Binary Systems

Toyota, Eri ; Itoh, Yoichi ; Ishiguma, Shinichiro ; Urakawa, Seitaro ; Murata, Daisuke ; Oasa, Yumiko ; Matsuyama, Hiroko ; Funayama, Hitoshi…

(Citation)
Publications of the Astronomical Society of Japan,61(1):19-28

(Issue Date)
2009-02-25

(Resource Type)
journal article

(Version)
Version of Record

(URL)
https://hdl.handle.net/20.500.14094/90001422

PASJ: Publ. Astron. Soc. Japan **61**, 19–28, 2009 February 25

Radial Velocity Search for Extrasolar Planets in Visual Binary Systems

Eri TOYOTA,[1] Yoichi ITOH,[1] Shinichiro ISHIGUMA,[1] Seitaro URAKAWA,[2] Daisuke MURATA,[1]
Yumiko OASA,[1] Hiroko MATSUYAMA,[1] Hitoshi FUNAYAMA,[1] Bun'ei SATO,[3] and Tadashi MUKAI[1]
[1]*Graduate School of Science and Technology, Kobe University, 1-1 Rokkodai, Nada-ku, Kobe 657-8501*
[2]*Bisei Spaceguard Center, Japan Spaceguard Association, 1716-3 Okura, Bisei-cho, Ibara, Okayama 714-1411*
[3]*Tokyo Institute of Technology, 2-12-1 Ookayama, Meguro-ku, Tokyo 152-8551*
toyota@kobe-u.ac.jp

(Received 2008 May 23; accepted 2008 September 3)

Abstract

We searched for extrasolar planets in visual binary systems using precise Doppler-shift measurements taken over a period of 4 yr. Using the HIgh Dispersion Echelle Spectrograph (HIDES) equipped on the Okayama Astrophysical Observatory (OAO) 188 cm reflector, we achieved a radial-velocity precision of about 10 m s^{-1}. We monitored both primary and secondary stars of six visual binary systems, and primary stars of three visual binaries. Among them, three objects show large radial-velocity variations. ADS 7311 A exhibits a decreasing trend in radial velocity with a best-fit slope of -30 m s^{-1} yr^{-1}, while 31 Dra A shows an increasing trend with a best-fit slope of $+220$ m s^{-1} yr^{-1}. These long-term trends in radial velocity may be attributable to unseen companions. BDS 10966 A shows a periodic variation in radial velocity with a period of 840 d and a semiamplitude of about 120 m s^{-1}, implying an association of a planetary-mass companion, rotational modulation, or nonradial oscillation of the photosphere. In any case, we should mention the nonassociation between BDS 10966 A and B, suggested by the different proper motions, radial velocities, and Hipparcos parallaxes.

Key words: stars: binaries: visual — stars: planetary systems — techniques: radial velocities

1. Introduction

Approximately 280 extrasolar planets have been discovered, and it is now considered that about 11% of stars have planets (Butler et al. 2006). These planets differ greatly from those in our solar system. For example, some bodies are Jupiter-mass planets whose orbits have very small semimajor axes, while others have very high orbital eccentricities.

While multiple star systems are common in the solar neighborhood (Duquennoy & Mayor 1991; Jahreiß & Wielen 2000), most of the planets discovered to date are associated with single stars. While we previously believed that a planet cannot survive in a binary system, an extensive theoretical study predicts that in a binary system with a large semimajor axis, a planet can exist stably for a long time (Holman & Wiegert 1999). For example, a planet is stable in an equal mass binary system with a circular orbit if the semimajor axis of the planet's orbit is less than one-fourth of the semimajor axis of the binary's orbit.

About 40 planets have been discovered in multiple star systems (Eggenberger et al. 2004; Konacki 2005a; Raghavan et al. 2006). Recent observational results suggest differences in orbital elements between the planets found around single stars and those in binary systems (Zucker & Mazeh 2000; Eggenberger et al. 2004; Desidera & Barbieri 2007). For planets whose periods are less than 40 d, an examination of the mass-period distribution reveals only two massive [minimum mass > 2 Jupiter mass ($M_{\rm J}$)] planets orbiting single stars (Wright et al. 2007; Fischer et al. 2007), and three such planets in binary systems. Eggenberger, Udry, and Mayor (2004) also found differences in the eccentricity–period distribution; especially, for the period range addressed above, planets in binary systems have very low eccentricities. These differences may suggest different formation and evolution processes of planets orbiting single stars and those in binary systems; however, more data from planets in binary systems are required to draw firm conclusions.

Two approaches are applied for detecting planets in binary systems. One is a search for stellar companions around a known planet hosting stars. This search is conducted by measuring proper motions using imaging data (e.g., Mugrauer et al. 2006). About 20 companions are confirmed around planet-hosting stars. The other method is a search for planets in known binary systems. This type of search is carried out mainly through the Doppler-shift method (e.g., Eggenberger et al. 2003; Gratton et al. 2003; Konacki 2005b). This method has detected about 15 planets in binary systems.

We searched for extrasolar planets in visual binary systems using precise Doppler-shift measurements obtained with the HIgh Dispersion Echelle Spectrograph (HIDES: Izumiura 1999) equipped on the Okayama Astrophysical Observatory (OAO) 188 cm reflector. We describe the targets in section 2 and discuss the observations and analysis methods in section 3. We present the results in section 4, discuss the radial velocity variations in section 5, and summarize our findings in section 6.

2. Target Stars

We selected 15 stars, 6 primaries and 6 secondaries in 6 binary systems and primary stars in 3 binary systems from the Washington Visual Double Star Catalog (Worley & Douglass 1997), using the following criteria:

Table 1. Target stars.

Object name	HD	HIP	V [mag]	Sp. types	Separation [arcsec]	a [AU]	π [mas]	$v \sin i$ [km s^{-1}]	Mass [$M_\odot$]	References*
ADS 3085 A	26923	19859	6.33	G0 IV			47.20	4.3	1.01	(a)(b)
ADS 3085 B	26913	19855	6.96	G5 IV	65.5	1400	47.86	3.9	0.87	(a)(b)
ADS 5166 Aa	46136 A	31158	6.26	F6 V			9.21	20.6	1.43	(a)(b)
ADS 5166 B	46136 B	31156	6.95	G8	20.0	2200	8.96	60		(b)
ADS 6190 A	60584	36817	5.83	F6 V			16.00	41	1.32	(b)(c)
ADS 6190 B	60585	36817	5.87	F6 V	9.6	260		41	1.37	(b)(c)
ADS 9728 A	139461	76603	6.48	F6 V			40.19	5.3		(d)
ADS 9728 B	139460	76602	6.50	F6 IV–V	11.9	300	44.4	6.8		(d)
ADS 14279 A	197964	102532	4.27	K1 IV			32.14	2.9		(e)
ADS 14279 B	197963	102531	5.14	F7 V	10.0	280	31.69	6.1	1.42	(b)(f)
31 Dra A	162003	86614	4.56	F5 IV–V			45.38	12.9	1.38	(a)(b)
31 Dra B	162004	86620	5.78	G0 V	30.3	600	44.80	6.2	1.05	(b)(f)
ADS 7311 A	80586	45811	4.81	G8 III–IV$_+$...	229.4	15800	13.39	4.8	2.32	(g)(h)
ADS 9559 A	135722	74666	3.47	G8 III	104.9	3800	27.94	1.2		(a)
BDS 10966A	203857	105637	6.45	K5 III	365.4	70000	3.54			

* (a) de Medeiros and Mayor (1999), (b) Nordström et al. (2004), (c) Desidera et al. (2006) (d) Fekel (1997), (e) Hale (1994), (f) Gondoin (1999), (g) Reiners and Schmitt (2003), (h) Allende Prieto and Lambert (1999).

- The apparent separation of the binary must be larger than 5″, otherwise it is difficult to separate the primary and secondary stars.
- Neither the primary nor the secondary is a spectroscopic binary, except for ADS 9728 A.
- The visual magnitudes of both components of the binary should be brighter than 7th magnitude, except for ADS 9559 B, in order to achieve a Doppler-shift precision better than 10 m s^{-1}.
- The stellar spectral type must be between F5 and K9. Early-type stars have large rotational velocities, preventing us from measuring the radial velocity precisely. Late-type stars are too faint to obtain enough photons.
- We do not select the binary if both components are classified as Luminosity Class I, II, or III.
- The declination must be larger than $-16°$, except for ADS 6190 A and B.
- We reject the system if it was already searched for planets (61 Cyg: Walker et al. 1995; 16 Cyg: Cochran et al. 1997).

Three secondary stars were not suitable for target stars, because each of them was faint, a rapid rotator, or an early-type star. The target stars are listed in table 1. The semimajor axes presented in the seventh column were calculated from the apparent separations.

ADS 9728 A is a known single-lined spectroscopic binary (SB1). For this target we investigated the presence of a planet by analyzing the periodicity in residuals between the observed radial velocities and the radial velocities expected from the binary's orbit.

3. Observations and Analysis

3.1. Observations

The radial velocity of each object in the visual binary system was measured every one or two months between 2003 March and 2007 November, The observed wavelength was 5000–6000 Å. Using a 200 μm (0.″76) width slit, we achieved a wavelength resolution of $\sim$70000. The integration time was 2–30 min, depending on the target brightness and weather conditions. We obtained S/N ratios of 100 to 200 for a 6th magnitude star with an exposure time of less than 30 min. We also observed 70 Vir and β Vir as radial-velocity standard stars; 70 Vir is known to be a planet-hosting star, and β Vir is stable in radial velocity.

To measure precise radial velocities, we used an iodine cell (I_2 cell: Kambe et al. 2002). The I_2 cell is a glass case containing I_2 vapor, which is heated during observations to a temperature of 55 ± 0.2°C. Since it is located at the entrance of HIDES, stellar spectra are obtained through the I_2 cell. We also used a photon monitor, which records the intensity of an object in the slit of HIDES every 3 s, and calculates a photon-weighted central exposure time.

To check the stellar activity, we also observed the Ca II H (3968.49 Å) line for all targets except for ADS 9728 A and B. Emission in this line indicates chromospheric activity due to stellar magnetism (Middelkoop 1982; Noyes et al. 1984). The observed wavelength was 3800–4600 Å. Using a 250 μm (0.″95) width slit, we achieved a wavelength resolution of $\sim$50000. We obtained spectra with S/N $\sim$20 at the line and S/N $\sim$100 at the continuum for a 30 min exposure of a 6th magnitude star.

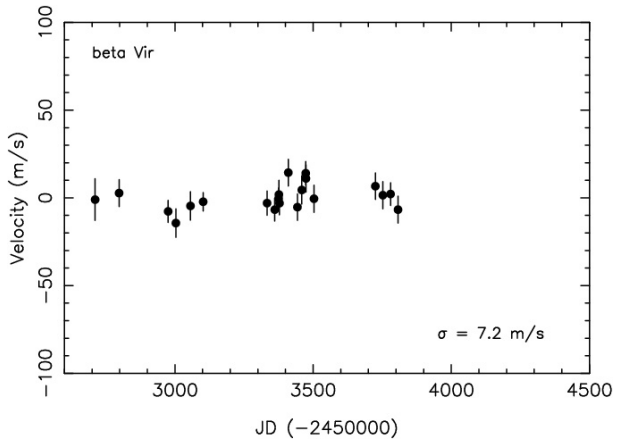

Fig. 1. Radial velocities of β Vir. The typical measurement error is $8\,\mathrm{m\,s^{-1}}$. The vertical axis represents the radial velocity and the horizontal Julian date; σ means the standard deviation of the radial velocity.

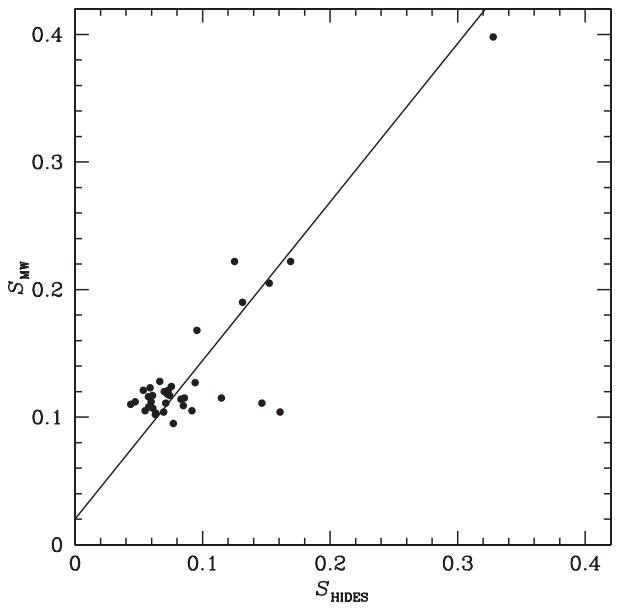

Fig. 2. Correlation between S_{HIDES} and S_{MW} systems.

3.2. *Analysis*

Reductions in the radial velocity data and the Ca II line data were performed by using the IRAF software package in the standard manner.

For the radial-velocity data, iodine lines superposed on the stellar spectra were used as a wavelength standard. The analysis method was based on Butler et al. (1996) and Valenti, Butler, and Marcy (1995). We used an analysis code optimized for the data taken with HIDES (Sato et al. 2002). We divided all spectra in the 5030 Å–5850 Å range into 5 Å segments, and analyzed all segments. The observed spectrum, $I(\lambda)$, was modeled as

$$I(\lambda) = k[A(\lambda)S(\lambda + \Delta\lambda)] * IP, \quad (1)$$

where $A(\lambda)$ is an iodine template spectrum, $S(\lambda)$ is an intrinsic stellar spectrum, and $\Delta\lambda = \lambda v/c$. Lambda, λ, represents the wavelength, v the radial velocity of the object, c the light speed, the sign $*$ the convolution, and IP the instrumental profile. The IP and the radial velocity are simultaneously determined by comparing the model spectrum with the observed spectrum by using least-squares fitting. An average of the radial velocity of individual segments is regarded as the radial velocity of a star.

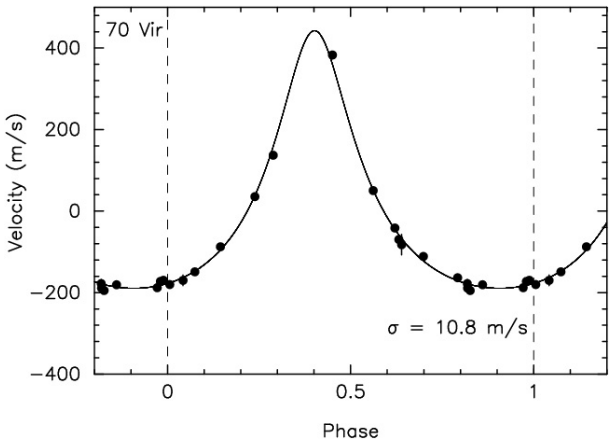

Fig. 3. Phased radial velocities of 70 Vir. The typical measurement error is 6–8 $\mathrm{m\,s^{-1}}$. The solid line represents the known orbital solution.

The strength of the Ca II H line emission is represented by an index, S. We measured the flux ratio, S_{HIDES}, between the emission core (3968.49 ± 0.5 Å) and the continuum (3996.50 ± 7.5 Å) (Santos et al. 2000), and then calibrated the activity index, S_{HIDES}, to the Mount Wilson S system (S_{MW}: Duncan et al. 1991). We made a conversion between these two systems from 35 stars observed by the program "Search for planets around G-type giants" (Sato et al. 2005). The correlation between the two systems is shown in figure 2 and the conversion is derived as

$$S_{\mathrm{MW}} = 1.242 S_{\mathrm{HIDES}} + 0.020 \quad (2)$$

with the rms of 0.01.

Next, we computed the fractional Ca II H and K flux corrected for the photospheric flux, R'_{HK} (Middelkoop 1982; Noyes et al. 1984). If $\log R'_{\mathrm{HK}}$ is larger than -4.8, the star's chromosphere is considered to be active (Henry et al. 1996). The Sun has low chromospheric activity, since $\log R'_{\mathrm{HK}}$ is -4.94. Note that the equations described above can be applied only to main-sequence stars.

4. Results

4.1. *Radial Velocity*

Beta Virginis is known to have a small radial velocity variation ($\sigma = 7.6\,\mathrm{m\,s^{-1}}$: Wittenmyer et al. 2006). Figure 1 shows the radial velocities of β Vir. The typical measurement error is $8\,\mathrm{m\,s^{-1}}$ and the standard deviation of the radial velocities for our measurements is $7.2\,\mathrm{m\,s^{-1}}$. We believe that this represents the long-term precision of the measurements. The radial velocities of 70 Vir are displayed in figure 3. This star is known to have a radial-velocity variation with a period of 116.7 d and

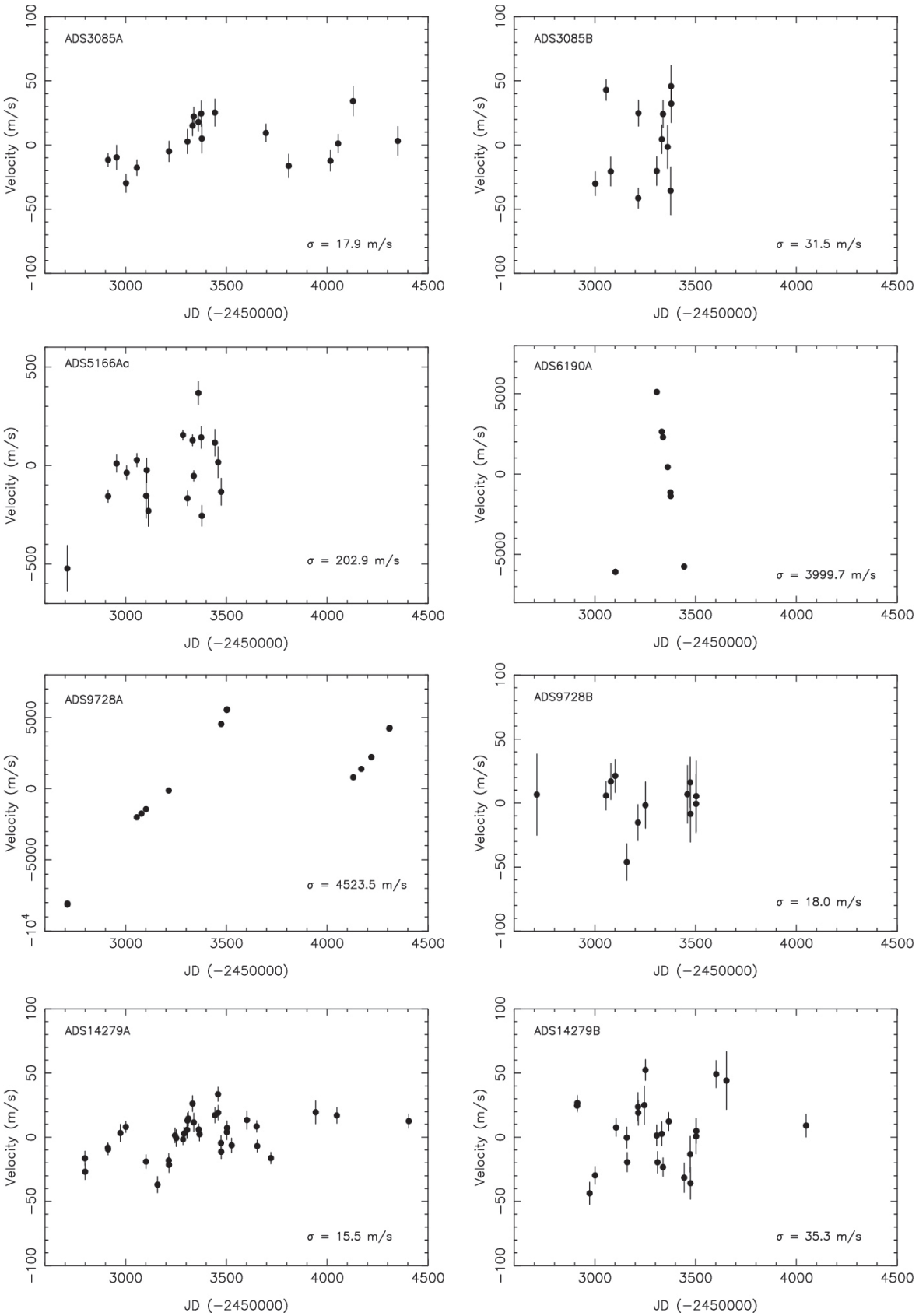

Fig. 4. Radial velocities of ADS 3085 A and B, ADS 5166 Aa, ADS 6190 A, ADS 9728 A and B, and ADS 14279 A and B.

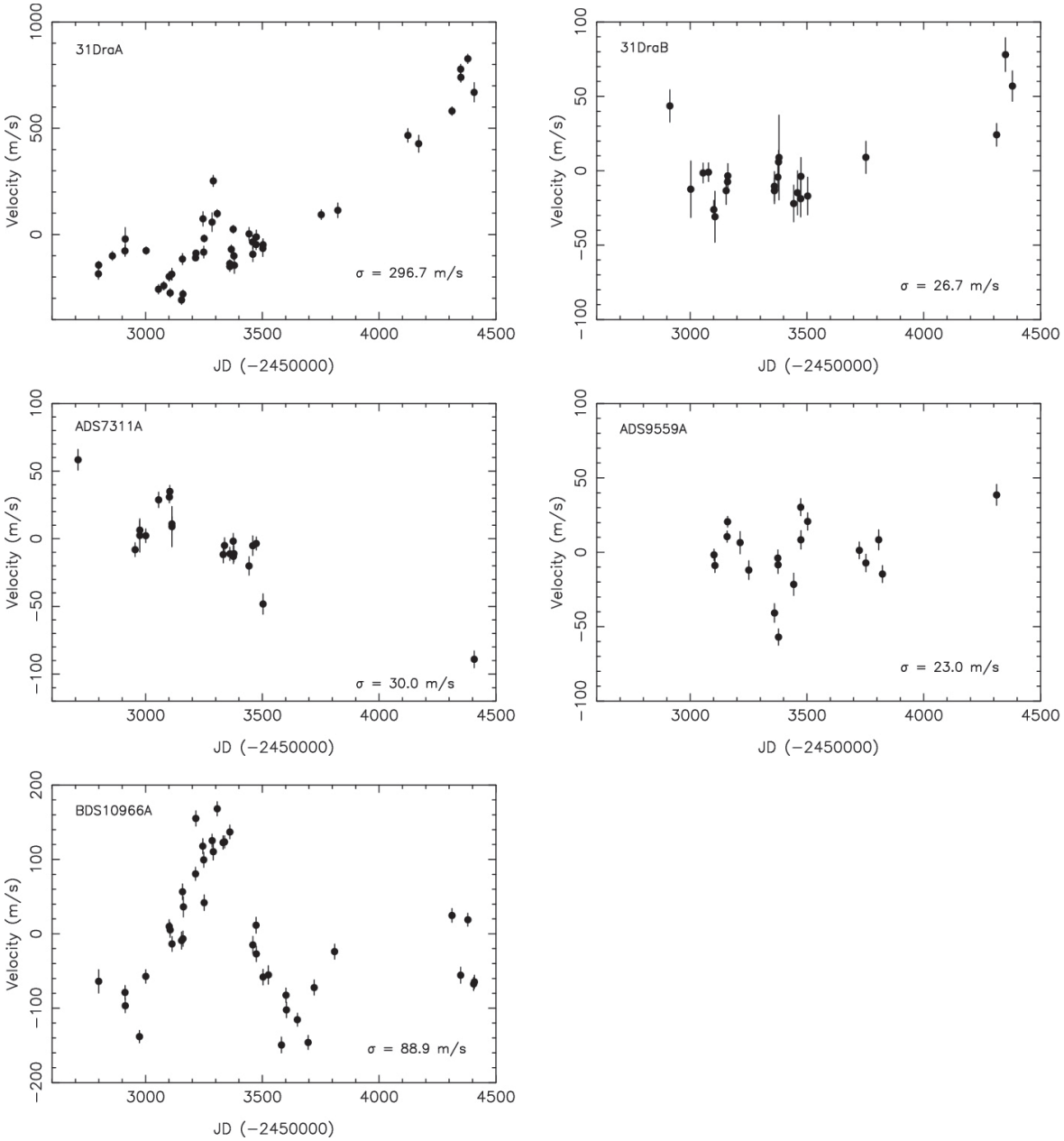

Fig. 5. Radial velocities of 31 Dra A and B, ADS 7311 A, ADS 9559 A, and BDS 10966 A.

an amplitude of 315 m s^{-1} that is caused by a planet (Marcy & Butler 1996; Butler et al. 2006). Our measurements of the radial velocities of this star are consistent with the orbital motion of the known planet.

We succeeded in measuring the radial velocity for 13 objects. The observed radial velocities are shown in figures 4 and 5 and table 2. We searched for periodicities among the radial velocities using a Lomb–Scargle periodgram (Lomb 1976; Scargle 1982). We also calculated false alarm probabilities (FAPs) of the highest peak in the periodgram with 10000 bootstrap randomizations (Kürster et al. 1997). We discuss our results below:

1. The standard deviations of the radial velocities of seven stars (ADS 3085 A, B; ADS 9559 A; ADS 9728 B; ADS 14279A, B; 31 Dra B) were smaller than 40 m s^{-1}, and their velocities show no significant periodic variations. The typical observation span was 1500 d. If a 1.8 $M_{\rm J}$ mass planet orbits the star with an orbital period of 1500 d, the semiamplitude of the radial velocity would be as large as 40 m s^{-1}. Thus, these observational results rejected the association of such a planet with the star. ADS 3085 A & B (HD 26923 and HD 26913) belong to the Ursa Major Moving Group, whose age is estimated to be 300 Myr (Soderblom & Mayor 1993). The large variations in the radial velocities and high S indices (table 3) may be attributed to a young age of the stars. Setiawan et al. (2004) measured the radial velocity of ADS 3085 A with an rms of 69 m s^{-1}. They did not

Table 2. Radial velocity measurements and periodgram analysis.*

Object name	N	Δ T [d]	σ [m s^{-1}]	$\overline{\text{Error}}$ [m s^{-1}]	Period [d]	Power	FAP [%]	$\sigma_{\rm lin}$ [m s^{-1}]	$\sigma_{\rm rot}$ [m s^{-1}]	$\sigma_{\rm ch}$ [m s^{-1}]
(1)	(2)	(3)	(4)	(5)	(6)	(7)	(8)	(9)	(10)	(11)
ADS 3085 A	18	1437	17.9	8.5	862.2	29	11.08		14.5	
ADS 3085 B	12	377	31.5	12.2	5.1	40	62.1		13.3	
ADS 5166 Aa	18	763	195.7	56.5	4.8	44	86.4		52.7	82.6
ADS 6190 A	8	341	3999.7	112.7	372.1	3800	$\leq$0.01		129.0	70.5
ADS 9728 A	14	1599	4523.5	17.1	—†	—	—		9.0	
ADS 9728 B	12	791	18.0	19.3	10.6	5.5	97.16		12.5	
ADS 14279 A	36	1607	15.5	5.7	11.3	40	64.78		10.2	
ADS 14279 B	25	1136	35.3	9.9	13.5	91	17.42		10.8	45.8
31 Dra A	42	1552	255.8	27.5	—†	—	—	132.7	28.7	
31 Dra B	22	1437	24.3	11.2	4.9	25	29.9		20.2	8.6
ADS 7311 A	21	1696	30.0	5.8	15.1	120	17.7	13.5		
ADS 9559 A	18	721	21.5	5.7	9.3	65	75.91			
BDS 10966 A	40	1609	88.9	11.5	839.4	1400	$\leq$0.01			

* (2) the number of observations; (3) observational span; (4) standard deviation of observed radial velocity; (5) the mean measurement error of the radial velocity; (7) power of the period; (8) false alarm probability for the period; (9) standard deviation of the residuals after linear fit; (10) radial velocity jitter expected from stellar rotation ($v \sin i$: Saar et al. 1998); (11) radial velocity jitter expected from chromospheric activity ($R'_{\rm HK}$: Saar et al. 1998).

† Periods of ADS 9728 A and 31 Dra A are much longer than our observational spans.

Table 3. Strength of the Ca II H emission lines.

Object name	$B-V$*	$S_{\rm MW}$ index	$\log R'_{\rm HK}$
ADS 3085 A	0.54	0.26	−4.18
ADS 3085 B	0.64	0.36	−4.16
ADS 5166 Aa	0.49	0.17	−4.37
ADS 5166 B	0.38	0.27	−4.36
ADS 6190 A	0.44	0.14	−4.41
ADS 6190 B	0.43	0.15	−4.37
ADS 14279 A	1.04	0.08	−4.45
ADS 14279 B	0.49	0.13	−4.52
31 Dra A	0.44	0.10	−4.63
31 Dra B	0.54	0.12	−4.70
ADS 7311 A	0.92	0.13	−5.73
ADS 9559 A	0.95	0.08	−5.51
BDS 10966 A	1.5	0.09	−6.27

* From the SIMBAD database.

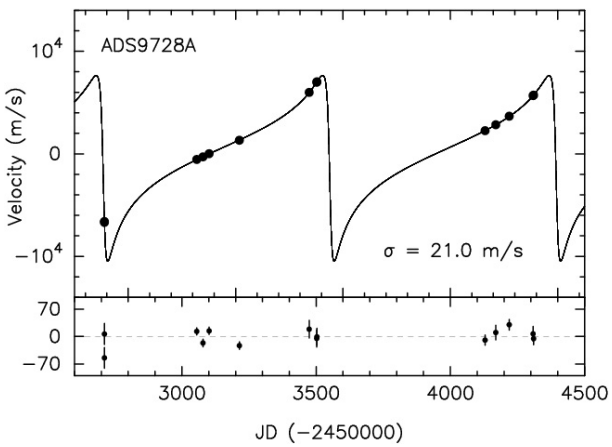

Fig. 6. Top: Radial velocity of ADS 9728 A. The solid line represents the orbital solution determined from the observed radial velocities. Bottom: Residuals after the Keplerian fit.

find any periodicity in the velocity. The rms of our measurements is about three times smaller than their rms, and our measurements are consistent with their result. Paulson and Yelda (2006) monitored the radial velocity of ADS 3085 B with an rms of 90 m s^{-1}. They did not find any periodicity in the velocity. Our result is consistent with their measurements. Wittenmyer et al. (2006) monitored the radial velocity of ADS 14279 A (γ^2 Del) during the period of 15 yr. The rms of the measurements is as small as 16.8 m s^{-1}, comparable to that of our measurements. They indicated a period of 3.837 d, but this periodicity is not secure because its FAP is as large as 0.099.

2. ADS 6190 A shows a large radial-velocity variation. Because the observed radial velocities varied between −5560 and +5640 m s^{-1}, the associated body is expected to be massive. We classify this star as a single-lined spectroscopic binary. Since the orbital period of this third body is considered to be longer than our observational span ($\sim$340 d), we cannot determine the orbital elements.
3. ADS 5166 Aa is a suggested spectroscopic binary (Wright et al. 2003), but its orbital elements are unknown. During our observational span, the observed radial velocities varied between −400 and +280 m s^{-1}. However, these velocities show no significant periodic variations.
4. ADS 9728 A is a known SB1 system (Tokovinin & Gorynya 2001, 2007: $P = 844.74 \pm 0.34$ d; a semi-amplitude, $K = 10.48 \pm 0.20$ km s^{-1}; $e = 0.835 \pm 0.006$; $\omega = 107\overset{\circ}{.}0 \pm 1\overset{\circ}{.}7$; the time of periastron passage,

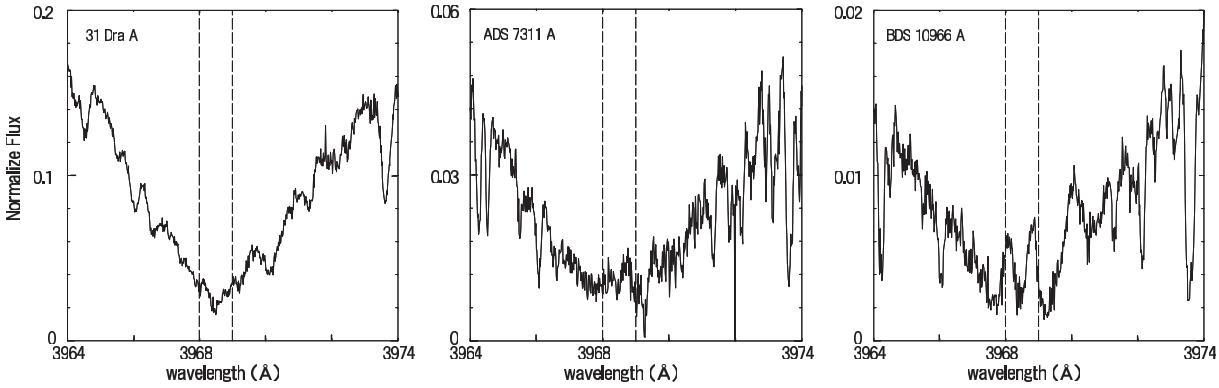

Fig. 7. Spectra of the Ca II H lines. The dashed lines represent the emission region of the spectra which is used to measure the activity index.

Table 4. Hipparcos photometry.

Object name (1)	HIP (2)	N (3)	ΔT (d) (4)	σ (5)	Period (d) (6)	Power (7)	FAP (%)
ADS 3085 A	19859	43	1123	0.007	8.8	11	0.53
ADS 3085 B	19855	44	1123	0.011	8.2	15	0.31
ADS 5166 Aa	31158	54	1078	0.129	5.0	590	≤0.01
ADS 5166 B	31156	43	1078	—	17.1	650	≤0.01
ADS 9728 A	76603	62	1065	0.064	56.3	51	3.57
ADS 9728 B	76602	60	1065	—	3.0	59	0.33
ADS 14279 A	102532	108	1009	0.036	3.0	220	1.84
ADS 14279 B	102531	108	1009	—	—*	—	—
31 Dra A†	86614	100	699	0.005	15.0	28	0.01
31 Dra B†	86620	107	700	—	4.0	31	0.15
ADS 7311 A	45811	98	1081	0.006	3.1	11	4.3
ADS 9559 A	74666	186	1081	0.004	4.8	16	1.52
BDS 10966 A	105637	197	1178	0.010	11.1	17	2.0

N, ΔT, and σ mean the same as in the table 2.
* Period of the ADS 14279 B is much longer than the observational span.
† Duplicity is cautioned in the photometry, which may degrade the photometric accuracy.

$T_{\rm peri} = 2451020.76 \pm 1.14$ d). We derived the orbital elements from the observed radial velocities as $P = 844 \pm 0.6$ d, $K = 9.1 \pm 0.4\,{\rm km\,s^{-1}}$, $e = 0.80^{+0.01}_{-0.00}$, $\omega = 101^\circ \pm 1^\circ$, and $T_{\rm peri} = 2451020.5 \pm 1$ d (figure 6). These orbital parameters agree reasonably well with theirs (Tokovinin & Gorynya 2007). The residuals of the radial velocity show no significant periodic variations.

5. The star 31 Dra A and ADS 7311 A exhibit linear trends. The star 31 Dra A shows an increasing trend in radial velocity, and the best fit has a slope of $+220\,{\rm m\,s^{-1}\,yr^{-1}}$. The best-fit slope for ADS 7311 A is $-30\,{\rm m\,s^{-1}\,yr^{-1}}$. Causes of these variations are discussed in the next section.
6. BDS 10966 A shows a large radial velocity variation. The standard deviation of its radial velocities is $90\,{\rm m\,s^{-1}}$. Causes of this variation are discussed in the next section.

For the other two targets, we could not measure the radial velocities with high precision due to their rapid rotations ($v \sin i = 60\,{\rm km\,s^{-1}}$ and $41\,{\rm km\,s^{-1}}$ for ADS 5166 B and ADS 6190 B, respectively) (Nordström et al. 2004; Desidera et al. 2006).

4.2. Ca II H Line

Figure 7 shows the Ca II H lines of 31 Dra A, ADS 7311 A, and BDS 10966 A. The very deep absorption (3960–3980 Å) is due to ionized calcium. ADS 7311 A and BDS 10966 A have moderate emissions; in contrast, 31 Dra A shows no emission at the center of the absorption. We present the S index and $\log R'_{\rm HK}$ in table 3. All dwarf stars are active compared to the Sun, and all giant stars (ADS 7311 A; ADS 9559 A; BDS10966 A) have moderate emissions in the Ca II H line. Note that Donahue, Saar, and Baliunas (1996) quoted a period of 7.15 d in the Ca II H and K emissions for ADS 3085 B.

4.3. Hipparcos Photometry

The variability of the radial velocities may arise from stellar pulsation or stellar magnetic activity. Indeed, some of the targets are rather active. ADS 3085 A and B are listed as BY Dra variables. We investigated the photometric variation of the targets, except for ADS 6190 A and B, using the Hipparcos photometric measurements. The results of Lomb–Scargle periodgram analysis are given in table 4. ADS 5166 Aa and

B may be variable stars. We found no significant periodicity in brightness of the other stars.

5. Discussion

5.1. Long-Term Trend in Radial Velocity

ADS 7311 A shows a decreasing trend in its radial velocity. The fit to the velocities has a slope of $-30\,\mathrm{m\,s^{-1}\,yr^{-1}}$. The residuals after the linear fit ($\sigma = 13.5\,\mathrm{m\,s^{-1}}$) show no significant periodic variation. We do not believe that the radial-velocity variation of ADS 7311 A is caused by the secondary star, ADS 7311 B. The semimajor axis of the ADS 7311 system is about 16000 AU. Since the period of the binary system ADS 7311 is longer than 1 million yr, the velocity change due to the secondary star is as small as $10^{-17}\,\mathrm{m\,s^{-1}\,yr^{-1}}$.

Instead, we assert that the radial-velocity variation is caused by another unseen companion. We estimated the companion mass by setting the first observation to be equal to the maximum radial velocity and the last to the minimum. Assuming a circular orbit, the semiamplitude, K, is about $80\,\mathrm{m\,s^{-1}}$. Since this observational span corresponds to half of the orbital period, $P = 3400$ d ($a \sim 5.9$ AU). Setting the mass of ADS 7311 A at $2.32\,M_\odot$ (Allende Priete & Lambert 1999), we deduced that the minimum mass of the unseen companion is about $10\,M_\mathrm{J}$.

We estimated the stability of the companion based on Holman and Wiegert (1999). The mass ratio of the ADS 7311 system is about 0.6, and its eccentricity is unknown. In the case where the orbit of the system is circular, the companion is stable if the semimajor axis of the companion's orbit is smaller than one-fourth of the semimajor axis of the binary's orbit. Thus, the companion is stable if its semimajor axis is smaller than about 3600 AU. Even if a system eccentricity of 0.8 is given, the companion is stable if the semimajor axis of the companion's orbit is smaller than $1/30$ of the semimajor axis of the binary's orbit (550 AU). Therefore, we believe that the companion of ADS 7311 A is stable. Note that the companion mass is $0.25\,M_\odot$ if the companion orbits at a distance of 3600 AU. Even if it is the case, we cannot find any absorption feature of the companion, because the difference in magnitude between the primary and the companion is as large as 11.5 mag at the V band.

We considered rotational modulation arising from a nonuniform surface as another possible explanation for the radial-velocity variation. The rotational velocity, v, of this star is $4.8\,\mathrm{km\,s^{-1}}$ (Reiners & Schmitt 2003), and the typical radius R of the G8 III–IV star is $\sim 8\,R_\odot$ (Fracassini et al. 1988). Using $T = 2\pi R/v$, we derived a rotational period T of ~ 80 d. This is much shorter than the observational span, and we did not detect such a period. Hence, we reject rotational modulation as the cause. Moreover, it is not likely that this radial-velocity variation is caused by oscillations whose period is longer than 1700 d. Such a long-term oscillation often occurs in Mira-type variable stars, but the spectral type of ADS 7311 A is G. Hence, we claim that this star has a high possibility of having an unseen companion. However, it is not yet known whether this companion is a planet, a brown dwarf, or a stellar-mass object.

The star, 31 Dra A, has radial-velocity variations larger than $500\,\mathrm{m\,s^{-1}}$, and the best linear fit to its velocity has a slope of $+220\,\mathrm{m\,s^{-1}\,year^{-1}}$. The residuals ($\sigma = 132.7\,\mathrm{m\,s^{-1}}$) do not show a significant periodic variation. Because the rotational period of the photosphere is 4.7 d (Hale 1994), much shorter than the observational span, the increasing trend of the radial-velocity variation is not induced by the rotational modulation arising from a nonuniform-surface feature. As previously noted, the long-term oscillation often occurs in Mira-type variable stars. However, 31 Dra A is an F5 star, allowing us to ignore the possibility that the radial-velocity variations are due to long-term oscillation.

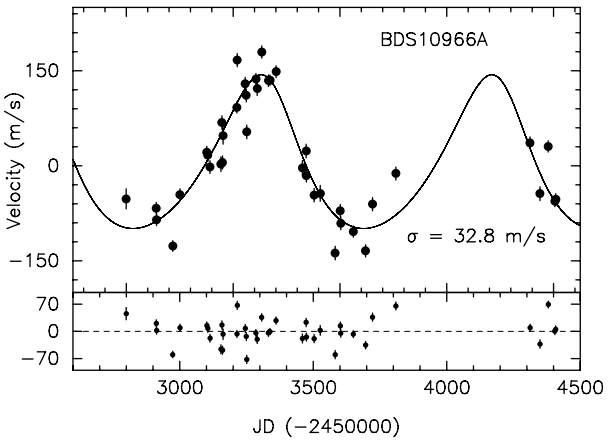

Fig. 8. Keplerian fit of the radial velocities of BDS 10966 A. We derived a period of 863.8 d, and a semiamplitude of $121\,\mathrm{m\,s^{-1}}$.

We do not consider that the radial-velocity variation of 31 Dra A is caused by the secondary star, 31 Dra B. The semimajor axis of the 31 Dra system is about 600 AU. Since the orbital period of the binary system is several thousand years, the velocity change due to the secondary star is about $10^{-12}\,\mathrm{m\,s^{-1}\,yr^{-1}}$. Another indication that we are not observing the binary motion of the wide pair is that in this case we would expect a similar slope with the opposite sign for the B component.

Instead, we maintain that 31 Dra A also has an unseen companion. We can estimate the companion mass using the above-mentioned procedure for ADS 7311 A. Setting the semiamplitude, K, at $550\,\mathrm{m\,s^{-1}}$ and the orbital period, P, at 3200 d ($a \sim 4.7$ AU), we estimate the minimum mass of the unseen companion to be about $50\,M_\mathrm{J}$. We can also apply the Holman and Wiegert stability criterion to the unseen companion. The mass ratio of the 31 Dra system is about 0.6, and its eccentricity is unknown. Assuming a circular orbit for the 31 Dra system, the companion exists stably if the semimajor axis of the companion is smaller than 140 AU. Assuming a system eccentricity of 0.8, a companion with a semimajor axis smaller than 18 AU is stable. Thus, we conclude that 31 Dra A has a stable companion. We notice that the use of a 2nd-order function improves the fit, though the residual is still large ($\sigma \sim 101.4\,\mathrm{m\,s^{-1}}$).

5.2. Periodic Variation of the Radial Velocity

BDS 10966 A has a large radial-velocity variation. A Keplerian fit gives a period of 863.8 d, a semiamplitude of $121.3\,\mathrm{m\,s^{-1}}$, and an eccentricity of 0.20 (figure 8). This

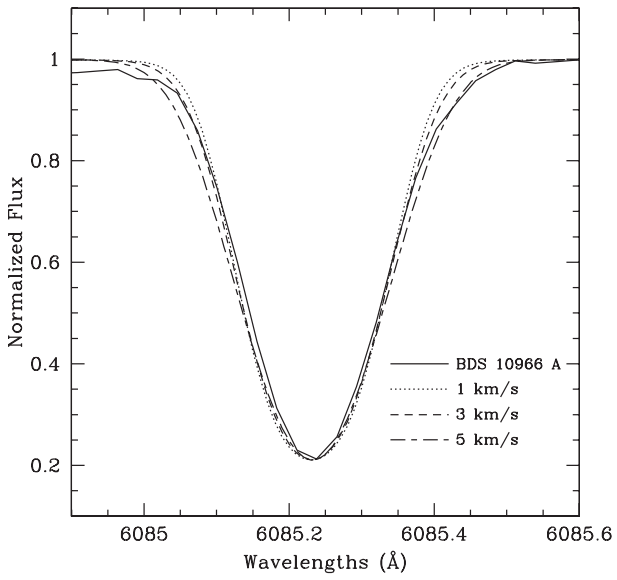

Fig. 9. Broadening of an absorption line depends on the rotational velocity. The solid line represents an absorption line (Fe II) of BDS 10966 A; the dot line corresponds to the rotational velocity of 1 km s^{-1}; the dashed line is that of 3 km s^{-1}; the dot-dashed line is that of 5 km s^{-1}.

variation may be induced by a low-mass companion or stellar activities. First, we considered an associated low-mass companion. The mass and semimajor axis of a companion can be estimated from the amplitude and the period of the variation, if the mass of the central star is known. The estimation of the mass of BDS 10966 A is as follows. Flower (1996) derived relationships between the colors, bolometric luminosities, and effective temperatures for giants. By the use of this relationship, the $B-V$ color of BDS 10966 A, 1.5 mag, corresponds to an effective temperature of 3980 K and a bolometric correction of -1.150. With $m_V = +6.45$ mag and $\pi = 3.54$ mas, $\log L/L_\odot$ is estimated to be 2.71. Based on an evolutionary track of Girardi et al. (2000), we estimated the mass of BDS 10966 A to be 1.7 $M_\odot$. Then, we estimated the mass ($m \sin i$) and semimajor axis of the associated planet to be 8.1 M_J and 2.1 AU, respectively. Thus, we may claim that a massive planet induces a radial-velocity variation.

However, the central star is an evolved K giant star (K5 III: Taylor 1999; Famaey et al. 2005). The radial-velocity variations of a giant star can be caused by either a low-mass companion, or stellar activities, such as oscillation and rotational modulation due to the surface inhomogeneity. K giant stars in particular are known to have long-period variations in the radial velocity due to such stellar activities (e.g., Hatzes & Cochran 1998). After a sinusoidal fit, BDS 10966 A shows a residual of 32.8 m s^{-1} in the radial velocity. The giants in Setiawan et al. (2004) with a similar color ($B-V = 1.5$ mag) show a variation of 60–140 m s^{-1}. Thus, the radial velocity of BDS 10966 A, itself, shows the amplitude that is typical of evolved stars, while its residuals after the sinusoidal fit would be rather anomalous.

Next, we considered stellar rotation, making synthesized spectra with SPTOOL (Takeda et al. 2002). The atmospheric parameters of BDS 10966 A were applied: an effective temperature of 3980 K and surface gravity of 1.30. We assumed [Fe/H] = 0.00. A typical microturbulent velocity of a giant with $\log g = 1.30$ is 2–3 km s^{-1} (Hekker & Meléndez 2007). We made models with a microturbulent velocity of 2 km s^{-1} and a rotational velocity ($v_{\rm rot} \sin i$) of 1, 3, and 5 km s^{-1} (figure 9). The shape of the absorption line of BDS 10966 A is consistent with that of a rotational velocity of 3 km s^{-1}. With this rotational velocity, the rotational period is calculated to be $\sim$800 d, which is consistent with the derived period of the radial velocity, 840 d. We noticed that the interstellar extinction toward BDS 10966 A is 0.14 mag at the V band (Famaey et al. 2005), with which the effective temperature changes into 4080 K. Even with this temperature, we derived the same rotational velocity. Thus, we can also claim that the radial velocity is caused by rotational modulation due to the surface inhomogeneity.

Then, we considered stellar pulsation. Integration of the Keplerian fit within the half period gives the amount of stellar radius variation due to the pulsation. We determined that the stellar radius varies between 46 and 50 $R_\odot$. Assuming no change in the effective temperature, we estimated that the magnitude varies by as much as 0.17 mag. However, Hipparcos photometric data show no such significant periodic variations (see table 4). Hence, we rejected the possibility of radial oscillation. Nevertheless, we could not rule out the possibility of nonradial oscillation.

Finally, we noticed that there are differences in proper motion, radial velocity, and parallax between BDS 10966 A and B. This wide binary system may not be a physical association, as pointed out by Wilson (1979).

5.3. Radial Velocity Jitter

Even after removing the stars with large velocity variations or considering the residuals from long-term trends, from table 2 it results that most of the stars have an rms dispersion larger than the internal errors. These scatters may be induced by low-mass companions, rotation modulations, or magnetic activities. Saar, Butler, and Marcy (1998) found empirical relations between the jitter of the radial velocity and the stellar rotation ($v_{\rm rot} \sin i$) and between the jitter and the Ca II H and K flux ($R'_{\rm HK}$) for F, G, and K dwarfs. We calculated the radial-velocity jitters expected from the stellar rotations and those from the chromospheric activities (table 2). By comparing with the standard deviations of the observed radial velocities, we claim that the magnetic activity is the primary cause of the radial-velocity variation for ADS 14279 B, and that rotational modulation is dominant in the radial-velocity variation of 31 Dra B.

Setiawan et al. (2004) observed a number of red giants, and found that the radial-velocity dispersion increases as a star evolves, though the reason for the variability is unknown. Both ADS 7311 A and ADS 9559 A in our sample have spectral types of G8 III. The radial-velocity variation of giants with a similar spectral type in Setiawan et al. (2004) is 20–60 m s^{-1}, comparable to the scatters of our two stars.

For the rest dwarfs, neither stellar rotation nor magnetic activity accounts for the whole amplitudes of the radial-velocity variations observed. We can consider that low-mass companions induce such variations. Further long-term monitoring of the radial velocities is strongly required.

6. Summary

Since 2003, we searched for extrasolar planets in 19 visual binary systems using precise Doppler-shift measurements. Over a period of 4 yr, by using β Vir as a standard star, we achieved a radial-velocity precision of better than $10\,\mathrm{m\,s^{-1}}$. Seven of the target stars exhibit a radial-velocity variation smaller than $40\,\mathrm{m\,s^{-1}}$ and without periodicity.

ADS 6190 A is a SB1. ADS 9728 A is known to be a SB1, and the radial-velocity residuals do not show any periodic variation. ADS 7311 A and 31 Dra A have long-term trends in radial velocity. We suggest unseen companions with periods longer than the observational span. The radial velocity of BDS 10966 A has a periodic variation. This variation is caused by an $8.1\,M_{\mathrm{J}}$ companion, rotational modulation, or nonradial oscillation of the photosphere. Further investigations, such as line bisector measurements, are needed to confirm whether the variations are due to a low-mass companion, to stellar rotation, or to nonradial photospheric oscillation. Finally, we noticed that different proper motions, radial velocities, and parallaxes between BDS 10966 A and B argue against a physical association of the two stars.

This research is based on data collected at Okayama Astrophysical Observatory (OAO), which are operated by National Astronomical Observatory of Japan (NAOJ). We thank all of the staff members at OAO for their support during the observations. Data analyses were in part carried out on the general common-use computer system at the Astronomy Data Center of NAOJ. This study was supported by "The 21st Century COE Program: The Origin and Evolution of Planetary Systems" of the Ministry of Education, Culture, Sports, Science and Technology. This research has made use of the SIMBAD database, operated at CDS, Strasbourg, France.

References

Allende Priete, C., & Lambert, D. L. 1999, A&A, 352, 555
Butler, R. P., et al. 2006, ApJ, 646, 505
Butler, R. P., Marcy, G. W., Williams, E., McCarthy, C., Dosanjh, P., & Vogt, S. S. 1996, PASP, 108, 500
Cochran, W. D., Hatzes, A. P., Butler, R. P., & Marcy, G. W. 1997, ApJ, 483, 457
de Medeiros, J. R., & Mayor, M. 1999, A&AS, 139, 433
Desidera, S., & Barbieri, M. 2007, A&A, 462, 345
Desidera, S., Gratton, R. G., Lucatello, S., Claudi, R. U., & Dall, T. H. 2006, A&A, 454, 553
Donahue, R. A., Saar, S. H., & Baliunas, S. L. 1996, ApJ, 466, 384
Duncan, D. K., et al. 1991, ApJS, 76, 383
Duquennoy, A., & Mayor, M. 1991, A&A, 248, 485
Eggenberger, A., Udry, S., & Mayor, M. 2003, ASP Conf. Ser., 294, 43
Eggenberger, A., Udry, S., & Mayor, M. 2004, A&A, 417, 353
Famaey, B., Jorissen, A., Luri, X., Mayor, M., Udry, S., Dejonghe, H., & Turon, C. 2005, A&A, 430, 165
Fekel, F. C. 1997, PASP, 109, 514
Fischer, D. A., et al. 2007, ApJ, 669, 1336
Flower, P. J. 1996, ApJ, 469, 355
Fracassini, M., Pasinetti-Fracassini, L. E., Pastori, L., & Pironi, R. 1988, Bull. d'Inf. Cent. Donnees Stellaires, 35, 121
Girardi, L., Bressan, A., Bertelli, G., & Chiosi, C. 2000, A&AS, 141, 371
Gondoin, P. 1999, A&A, 352, 217
Gratton, R., et al. 2003, ASP Conf. Ser., 294, 47
Hale, A. 1994, AJ, 107, 306
Hatzes, A. P., & Cochran, W. D. 1998, MNRAS, 293, 469
Hekker, S., & Meléndez, J. 2007, A&A, 475, 1003
Henry, T. J., Soderblom, D. R., Donahue, R. A., & Baliunas, S. L. 1996, ApJ, 111, 439
Holman, M. J., & Wiegert, P. A. 1999, AJ, 117, 621
Izumiura, H. 1999, in Proc. 4th East Asian Meeting on Astronomy, ed. P. S. Chen (Kunming:Yunnan Observatory), 77
Jahreiß, H., & Wielen, R. 2000, IAU Symp., 200, 129
Kambe, E., et al. 2002, PASJ, 54, 865
Konacki, M. 2005a, ApJ, 626, 431
Konacki, M. 2005b, Nature, 436, 230
Kürster, M., Schmitt, J. H. M. M., Cutispoto, G., & Dennerl, K. 1997, A&A, 320, 831
Lomb, N. R. 1976, Ap&SS, 39, 447
Marcy, G. W., & Butler, R. P. 1996, ApJ, 464, L147
Middelkoop, F. 1982, A&A, 107, 31
Mugrauer, M., Seifahrt, A., Neuhäuser, R., & Mazeh, T. 2006, MNRAS, 373, L31
Nordström, B., et al. 2004, A&A, 418, 989
Noyes, R. W., Hartmann, L. W., Baliunas, S. L., Duncan, D. K., & Vaughan, A. H. 1984, ApJ, 279, 763
Paulson, D. B., & Yelda, S. 2006, PASP, 118, 706
Raghavan, D., Henry, T. J., Mason, B. D., Subasavage, J. P., Jao, W.-C., Beaulieu, T. D., & Hambly, N. C. 2006, ApJ, 646, 523
Reiners, A., & Schmitt, J. H. M. M. 2003, A&A, 398, 647
Saar, S. H., Butler, R. P., & Marcy, G. W. 1998, ApJ, 498, L153
Santos, N. C., Mayor, M., Naef, D., Pepe, F., Queloz, D., Udry, S., & Blecha, A. 2000, A&A, 361, 265
Sato, B., Kambe, E., Takeda, Y., Izumiura, H., & Ando, H. 2002, PASJ, 54, 873
Sato, B., Kambe, E., Takeda, Y., Izumiura, H., Masuda, S., & Ando, H. 2000, PASJ, 57, 97
Scargle, J. D. 1982, ApJ, 263, 835
Setiawan, J., Pasquini, L., da Silva, L., Hatzes, A. P., von der Lühe, O., Girardi, L., de Medeiros, J. R., & Guenther, E. 2004, A&A, 421, 241
Soderblom, D. R., & Mayor, M. 1993, AJ, 105, 226
Takeda, Y., Ohkubo, M., & Sadakane, K. 2002, PASJ, 54, 451
Taylor, B. J. 1999, A&AS, 134, 523
Tokovinin, A. A., & Gorynya, N. A. 2001, A&A, 374, 227
Tokovinin, A. A., & Gorynya, N. A. 2007, A&A, 465, 257
Valenti, J. A., Butler, R. P., & Marcy, G. W. 1995, PASP, 107, 966
Walker, G. A. H., Walker, A. R., Irwin, A. W., Larson, A. M., Yang, S. L. S., & Richardson, D. C. 1995, Icarus, 116, 359
Wilson, R. H., Jr. 1979, A&AS, 35, 193
Wittenmyer, R. A., Endl, M., Cochran, W. D., Hatzes, A. P., Walker, G. A. H., Yang, S. L. S., & Paulson, D. B. 2006, AJ, 132, 177
Worley, C. E., & Douglass, G. G. 1997, A&AS, 125, 523
Wright, C. O., Egan, M. P., Kraemer, K. E., & Price, S. D. 2003, AJ, 125, 359
Wright, J. T., et al. 2007, ApJ, 657, 533
Zucker, S., & Mazeh, T. 2002, ApJ, 568, L113